Developments for Cornell's X-Ray ERL

J. A. Crittenden, [*] I.V. Bazarov, S.A. Belomestnykh, D.H. Bilderback, M.G. Billing, J.D. Brock,
E.P. Chojnacki, B.M. Dunham, M.P. Ehrlichman, M.J. Forster, S.M. Gruner, G.H. Hoffstaetter,
C.J. Johnstone[†], Y. Li, M.Liepe, C.E. Mayes, A.A. Mikhailichenko, H.S. Padamsee, S.B Peck,
D.C. Sagan, V.D. Shemelin, A. Temnykh, M. Tigner, V. Veshcherevich
CLASSE, Cornell University, Ithaca, NY 14853-8001

Abstract

Cornell University is planning to build an Energy-Recovery Linac (ERL) X-ray facility. In this ERL design, a 5-GeV superconducting linear accelerator extends the CESR ring which is currently used for the Cornell High Energy Synchrotron Source. Here we describe some of the recent developments for this ERL, including linear and nonlinear optics incorporating the existing CESR lattice elements and a dual turnaround, undulator developments, optimization of X-ray beams, progress in calculations of coherent synchrotron radiation, and the technical design of ERL cavities and cryomodules.

INTRODUCTION

The potential for excellent quality of X-ray beams from low-emittance electron beam produced by a 5-GeV superconducting energy-recovery linac (ERL) is motivating an intensive development study at the Cornell Laboratory for Accelerator-based Sciences and Education (CLASSE). Table 1 compares the ERL design parameters to those of existing light sources. We report on design progress achieved since EPAC08 [1].

Table 1: The approximate particle energy, average current, horizontal emittance, and bunch length for the proposed Cornell ERL along with existing light source facilities.

Name	Energy (GeV)	Current (mA)	Emittance (pm-rad)	σ_z/c (ps)
ESRF	6	200	4000	20
APS	7	100	2500	20
SPring 8	8	100	3000	13
ERL mode A	5	100	30	2
mode B	5	25	8	2
mode C	5	1	500	0.1

OPTICS

The present status of the ERL layout and X-ray beamlines is shown in Fig. 1. A detailed description of the optics design principles, methods, and results can be found in Ref. [2]. Optics design constraints include preservation of the small beam size and emittance and controlling the

_____
[*] crittenden@cornell.edu
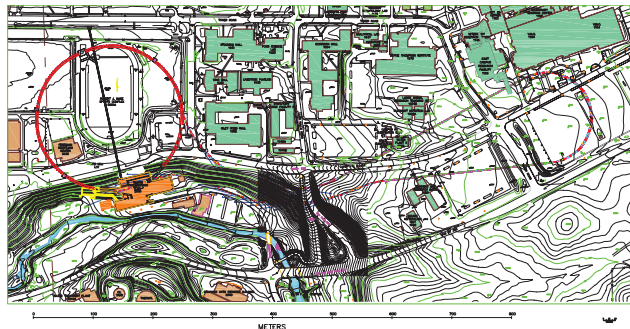[†] Fermi National Accelerator Laboratory, Batavia, IL 60510

Figure 1: Proposed layout of the 5-GeV superconducting X-ray energy recovery linac design on the Cornell campus map

first and second-order dispersion and time-of-flight terms throughout the undulator arcs providing the X-ray beamlines. The dual-pass sections of the ERL, such as the linacs and the matching sections into the dual turnaround require simultaneous optics optimization at two beam energies. These purposes are served by the TAO accelerator simulation package which remains under active development at Cornell [3]. The capability of this software utility has been recently upgraded with features useful for the design of ERL-based light sources: 1) multi-pass beamline elements and tracking, 2) tracking calculations of beam breakup stability thresholds, 3) wakefield calculations, 4) modeling of coherent synchrotron radiation and intra-beam scattering, 5) simultaneous optics optimizations for multiple beams, 6) spurs for extracted beams, and 7) X-ray beamline design. The optimization procedure is highly modular, allowing quick, convenient re-optimization of subsections of each the linac, turnaround, arc and CESR sections. The complete beta functions and dispersion, including the energy recovery pass, are shown in Fig. 2.

North and South Linacs and Dual Turnaround

The linac sections comprised of superconducting RF (SRF) cavities, quadrupoles, and steering correctors, have been redesigned such that the first- and second-pass beams pass through the new dual turnaround with differing energies. The high-energy North Linac (LA) now accelerates/decelerates the beam by 2.8 GeV in 36 cryomodules, while the South Linac (SA) is comprised of 28 such cryomodules. This configuration will permit wake field compensation as described in Ref. [4]. Figure 3 shows the re-
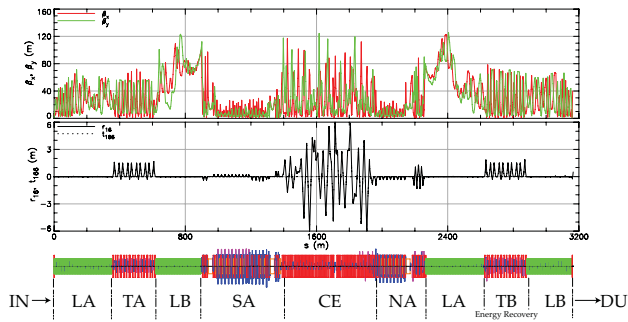
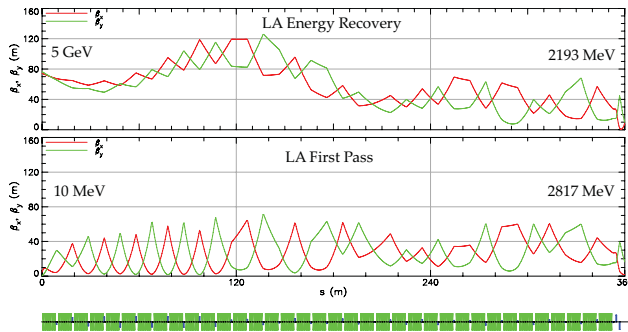Figure 2: Dual-pass beta functions and dispersion

Figure 3: Beta functions for the first pass (accelerating) beam and energy-recovery (decelerating) beam in LA
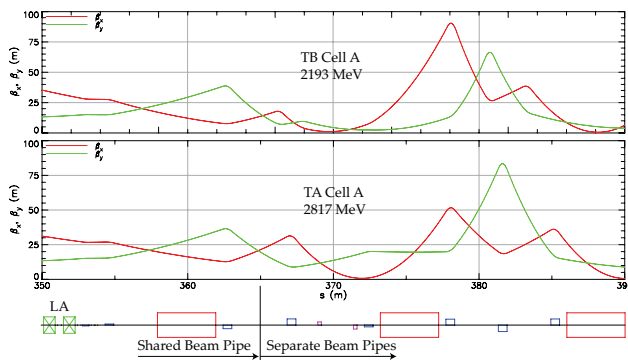

Figure 4: Beta functions for the high- and low-energy turnaround entrance cells

CESR and the South and North Arcs

The layout of the North and South Arcs (NA, SA) and the X-ray beamlines in the proposed new laboratory building is shown in Fig. 5. The first of the nine undulators in the South Arc and the last of the eight undulators in the NA are 25 m long. The rest are 5 m long. The opti-
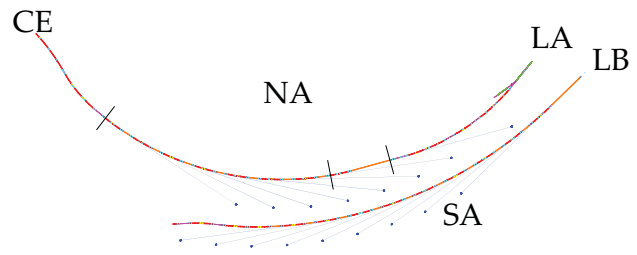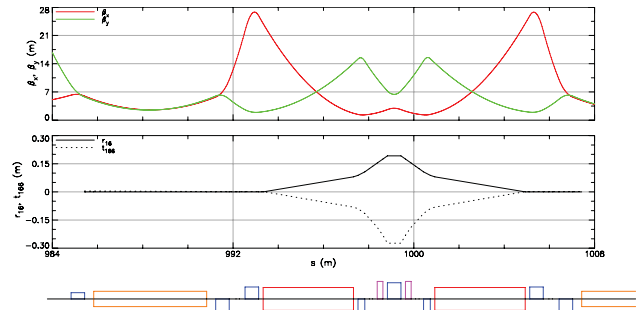

Figure 5: Layout of the North and South Arcs

Figure 6: Beta functions and first- and second-order dispersion in the 5-m undulator sections in the NA and SA.

cal design of the SA cells containing 5-m undulators begins with the undulator followed by a two-bend achromat. The bends provide an angle between the beginning and end of the cell so that the beamlines emitted from the undulators of consecutive cells have sufficient clearance from the shielding wall after 30 m to equip the X-ray beamlines. The Twiss parameters at the beginning and the end of the cell are fixed by the requirements of prior and succeeding undulators, where the vertical and horizontal beta functions are chosen to be equal to half the length of the undulator at its center. Seven quadrupole magnets, arranged symmetrically about the center of the achromat, are used to match these requirements, with the center three additionally used to focus the dispersion and its slope to zero at the end of the second bend. As with the previous sections, emittance growth is reduced as much as possible while maintaining the Twiss parameter and dispersion requirements. Two sextupole magnets placed symmetrically about the center of the achromat are used to make the cells achromatic to second order through the two bends. The result of the optics optimization for such an undulator cell in the SA is shown in Fig. 6.

These NA and SA sections have been matched to the elements in the existing CESR layout. About 70% of the CESR ring is used. The first- and second-order CESR optics have been redesigned to meet Twiss, time-of-flight and second-order dispersion criteria. The resulting emittance growth, shown in Fig. 7, is vey small in the SA and only significant in the CE section. However, the existing CESR element layout is not sufficient to permit operation in the bunch compression mode C, which will be available in an extension to the SA, or following a custom upgrade of the

sulting beta functions for the NA. The optimization criteria keep the beta functions small and match the low-energy beam to the Twiss parameters from the injector. The beta functions of the entrance sections of the two turnarounds (high-energy TA and low-energy TB) are shown in Fig. 4. The two passes in these sections are optimized simultaneously to match into their respective distinct arcs.
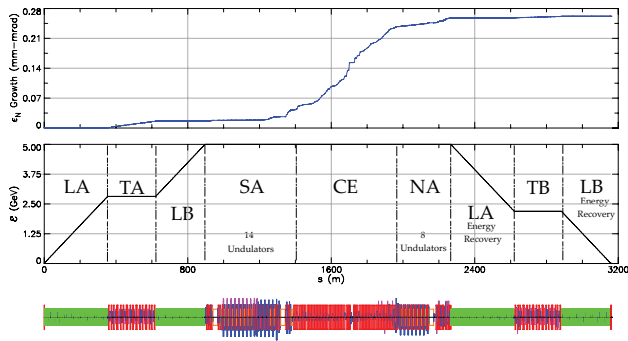
Figure 7: Radiative emittance growth ϵ_N and total energy $\mathcal{E}$ including the energy recovery pass.

magnet layout in the CESR ring.

Coherent Synchrotron Radiation

The minimum bunch length which can be achieved in the ERL is limited by the sum of the wake fields. A primary consideration for the 100-fs bunch length planned for the bunch-compression mode C is the contribution of wake fields from coherent synchrotron radiation. Significant progress has been made in developing calculational methods for quantifying this contribution, enabling the investigation of various shielding effects [5, 6].

RF CAVITY AND CRYOMODULE DESIGN

The cw duty factor and low emittance drive the choice to use SRF technology. The cryomodule for the ERL will be based on TTF technology, but must have several unique features dictated by the ERL beam parameters. The main deviations from TTF are that the HOM loads must be on the beamline for sufficient damping, that the average power through the RF couplers can be as low as 2 kW, and that cw beam operation introduces higher cryogenic heat loads. Much has been learned from the design, construction and commissioning of the cryomodule for the prototype ERL injector now in operation [7, 8]

The SRF cavities must have low RF losses to minimize refrigeration and strong HOM damping to preserve low emittance and prevent beam breakup [9]. A design to meet these requirements has been developed [10].

UNDULATOR DEVELOPMENT

A novel design for a compact, 30-cm-long, 5-mm round bore undulator with full X-ray polarization control has been optimized for use at the Cornell ERL and a prototype built [11]. The newly developed technique for soldering NdFeB permanent magnet blocks allows a 40% (100%) stronger magnetic field in linear (circular) polarization mode as compared to existing undulators with similar gap. The magnetic field strength is controlled by relative longitudinal adjustment of the two magnet arrays, as is the X-ray polarization control.

X-RAY BEAMLINES

Space has been allotted for four beamlines in Wilson Lab, including preserving the existing G-line and introducing a new 25-m undulator. The ERL can thus accommodate three 25-m undulators and nineteen 5-m undulators.

A variety of X-ray beam-line design projects are underway. These include a diffraction-limited scattering line, a short pulse/cw line, an ultra-short pulse, high-repetition-rate line for time-resolved scattering and spectroscopic structural studies, a highly coherent, high-flux line for diffractive imaging and dynamics studies of bulk materials, interfaces and biological samples, as well as a beamline for meV-resolution inelastic X-ray scattering.

CONCLUSION

The conceptual design for a dual-pass energy-recovery-linac-based X-ray source at Cornell is under active development. Complete linear and second-order optics have been designed incorporating the existing CESR ring and optical elements, and a dual-turnaround scheme for wake field compensation has been included. Progress has been made in the design of X-ray beamlines. A novel design for an undulator which controls X-ray polarization is in the prototyping stage. Many ongoing aspects of the design effort exceed the scope of this report, including vacuum design, instrumentation, siting issues, intra-beam scattering estimates, beam breakup computations, as well as work on collimation and shielding. Much is yet to be learned from operation of the injector prototype as progress continues toward a complete conceptual design report.

REFERENCES

[1] G.H. Hoffstaetter *et al.*, *Progress Toward An ERL Extension To CESR*, proceedings of EPAC08

[2] C.E. Mayes, Ph.D. Dissertation, Cornell University (2009)

[3] D. Sagan and J.C. Smith, *The TAO Accelerator Simulation Program*, proceedings of PAC05

[4] G.H. Hoffstaetter and Y.H. Lau, Phys. Rev. ST-AB **11**, 070701, 2008

[5] C.E. Mayes and G.H. Hoffstaetter, Phys. Rev. ST-AB **12**, 024401,2009

[6] D.C. Sagan, G.H. Hoffstaetter, C.E. Mayes, and U. Sae-Ueng, Phys. Rev. ST-AB **12**, 040703 (2009)

[7] E.P. Chojnacki *et al.*, *Design of an ERL Linac Cryomodule*, these proceedings

[8] I.V. Bazarov, *et al.*, *Initial Beam Results from the Cornell High-Current ERL Injector Prototype*, these proceedings

[9] G.H. Hoffstaetter and I.V. Bazarov, Phys. Rev. ST-AB **7**, 054401 (2004), G.H. Hoffstaetter, I.V. Bazarov and C. Song, Phys. Rev. ST-AB **10**, 044401 (2007)

[10] M. Liepe, *SRF Experience with the Cornell High-Current ERL Injector Prototype*, these proceedings

[11] A. Temnykh, *Delta Undulator Magnet for Cornell Energy Recovery Linac*, these proceedings